Environmental Science: Atmospheres

ROYAL SOCIETY OF CHEMISTRY

PAPER

View Article Online
View Journal | View Issue

Cite this: *Environ. Sci.: Atmos.*, 2022, **2**, 375

Photo-enhanced uptake of SO_2 on Icelandic volcanic dusts†

Jerome Lasne, *[a] Darya Urupina,[a] Elena C. Maters, [b] Pierre Delmelle,[c] Manolis N. Romanias *[a] and Frederic Thevenet[a]

Iceland is the largest volcanic dust (v-dust) desert on Earth, with an estimated area of 22 000 km^2. In addition, Iceland is one of the most active aeolian areas in the world, with frequent high-velocity winds resuspending v-dust from the ground into the atmosphere. Suspended v-dust particles can then be transferred over thousands of kilometers, reaching as far as central Europe. Once released into the atmosphere, v-dust particles can interact or react with atmospheric pollutants. In this study, we investigate the heterogeneous reactivity of sulfur dioxide (SO_2), one of the most prominent gases released by volcanic eruptions, with Icelandic v-dust particles, and the influence of relevant atmospheric parameters, such as relative humidity (RH) and ultraviolet (UV) light flux, on this reactivity. The experiments are conducted at atmospheric pressure in a coated-wall flow-tube reactor coupled with an SO_2 analyzer. To quantify the heterogeneous processes, we determine the initial number of SO_2 molecules taken up by dust, N_S, and the steady-state uptake coefficient, γ_{ss}, of SO_2 on different v-dusts. N_S increases with RH and with the photon flux characterized by the photolysis rate of NO_2 in the setup, J_{NO_2}. The photo-enhanced removal of SO_2 is also found to depend on the surface elemental composition of v-dust particles, and an empirical parametrization of the photo-induced effect is proposed to account for the most important environmental factors, leading to the general expression: $N_{S,light}/N_{S,dark} = 6.1 \times (1 + 7.76 \times 10^{-2} \times RH) \times (1 + 480.5 \times J_{NO_2}) \times (Ti/Si)$. The steady-state uptake coefficients of SO_2 are in the 10^{-8} range, once normalized to the specific surface area of v-dust. RH and UV light influence the value of γ_{ss}, but to a lesser extent than they influence N_S. Our results suggest that the photo-induced heterogeneous uptake of SO_2 on v-dust particles may provide a significant sink of sulfur in volcanic clouds, and should be taken into account in atmospheric modeling.

Received 15th November 2021
Accepted 7th February 2022

DOI: 10.1039/d1ea00094b

rsc.li/esatmospheres

Environmental significance

SO_2 is an atmospheric pollutant that plays a key role in the environment. It is well established in the literature that SO_2 can interact/react with atmospheric particles. However, there is limited knowledge on SO_2 interaction with natural volcanic particles, despite the significance of this heterogeneous process on air quality and climate. In this study, we investigate the heterogeneous uptake of SO_2 on natural volcanic particles. Using a well-established experimental approach, the SO_2 uptake coefficients and surface coverages are determined under atmospheric levels of relative humidity (RH) and light radiation. A multi-parametric equation is developed and applied to fit SO_2 removal on volcanic particles.

1. Introduction

Volcanic eruptions are a highly variable source of solid particles; annual emissions of fine volcanic ash (<63 μm) are estimated between 176 and 256 Tg on average,[1] accounting for 5.1–7.4% of total aerosol emissions.[2] Iceland is a very active geological site that features volcanic eruptions typically every 3 to 5 years,[3] and thus it is a major source of volcanic particles in the atmosphere. The Eyjafjallajökull eruption in 2010 emitted 8.3 ± 4.2 Tg of fine ash in the 2.8–28 μm diameter range, as determined by inverse modeling of satellite observations.[4] Ash subsequently settles on the ground, we refer to this material as volcanic dust (hereafter 'v-dust'), and can be remobilized by the strong winds that cause frequent dust storm events in Iceland.[5] It is estimated that around 30 to 40 Tg of Icelandic v-dust is resuspended annually.[5] The dust event observed in september 2013 in Southern Iceland was composed of remobilized ash from the 2010 Eyjafjallajökull and 2011 Grimsvötn eruptions, and accounted for roughly 0.2 Tg

[a]*IMT Nord Europe, Institut Mines-Télécom, Univ. Lille, CERI EE, F-59000 Lille, France. E-mail: jerome.lasne@imt-nord-europe.fr; emmanouil.romanias@imt-nord-europe.fr; Tel: +33 3 27 71 26 33; +33 3 27 71 22 93*

[b]*Department of Chemistry, University of Cambridge, Lensfield Road, Cambridge CB2 1EW, UK*

[c]*Environmental Sciences, Earth & Life Institute, UCLouvain, Croix du sud 2, B-1348 Louvain-la-Neuve, Belgium*

† Electronic supplementary information (ESI) available. See DOI: 10.1039/d1ea00094b

of dust over the two days of observations.[6] Icelandic v-dust can travel thousands of kilometers before eventually being deposited. For instance, recent studies have observed the transportation of v-dust to the central Balkans.[7] Interestingly, v-dust exhibits thermal and optical properties similar to black carbon.[8] In general, volcanic particles play an important role in climate and can impact directly or indirectly the energy budget of the planet.[1,9–12]

In addition to particles, explosive volcanic eruptions release sulfur dioxide (SO_2) along with a range of other gases, among which water and carbon dioxide dominate.[1] Non-eruptive outgassing is a less spectacular, but continuous source of tropospheric volcanic gases. Typical concentrations of SO_2 in the plume range from 100 ppb (part per billion) to 3000 ppb.[13] Measurements while flying through the eruptive plume of Mount Hekla in 2000 recorded SO_2 concentrations up to 1000 ppb, with a large spatial variation at the edge of the cloud.[14] Observations of the plume of the Eyjafjallajökull volcano in 2010 showed average SO_2 mixing ratios of 40 ppb.[15]

SO_2 is an atmospheric species that plays a key role in the environment. The tropospheric background concentration of SO_2 is very low (ppt range),[16] and thus volcanic SO_2 emissions receive great attention. Once released into the atmosphere, SO_2 can either be (i) oxidized in the gas phase by hydroxyl radicals to produce sulfuric acid (H_2SO_4), a relatively minor atmospheric sink of SO_2, or (ii) dissolved in water droplets and oxidized by hydrogen peroxide, ozone or oxygen to form sulfate (SO_4^{2-}) species, which is a relatively fast atmospheric process. This conversion of SO_2 in the troposphere can affect human health and air quality,[17–19] as well as the radiative balance of the Earth due to the formation of sulfate aerosols.[19] SO_2 can also interact/react with airborne solid particles, especially during high particle loading, but this atmospheric process has received less attention than the gas and liquid phase oxidation of SO_2. Several literature studies have evidenced the uptake of SO_2 on mineral surrogates[20] and natural mineral dusts.[21,22] Reactions of SO_2 on desert and volcanic origin particles during dust storms could potentially impact the sulfur budget in the troposphere, but this heterogeneous transformation of SO_2 has not been yet fully assessed in the literature. The interaction of SO_2 with volcanic material (*i.e.*, ash or v-dust) is of particular interest due to the coexistence of high atmospheric loadings of particles and SO_2. Maters *et al.* measured the uptake of SO_2 on natural volcanic ash and synthetic volcanic glass samples under tropospherically relevant conditions of SO_2 concentration and temperature, but under dry conditions.[23] Recently, we have investigated for the first time the transformation of SO_2 on Icelandic v-dust;[24,25] we expand this work here by evaluating the uptake of SO_2 on v-dusts in the dark and under UV light irradiation. In particular, the aging of v-dusts by SO_2 is investigated under atmospherically relevant conditions, *i.e.*, at atmospheric pressure, an SO_2 concentration of 75 ppb, relative humidity (RH) in the 0–72% range, and in the dark and under different UV photon fluxes, performing long laboratory experiments over timescales of typically 24 hours. As a result, we quantify the initial number of SO_2 molecules taken up (N_S) and the steady-state uptake ($\gamma_{ss,BET}$) of SO_2 by Icelandic v-dust.

2. Methods

2.1 Materials

2.1.1. Dust samples origin and characterization. The v-dust samples originate from four areas of Iceland: Mýrdalssandur (63°26′50.1″N, 18°48′52.8″W), Dyngjusandur (64°50′41.885″N, 16°59′40.78″W), Hagavatn (64°28′6.12″N, 20°16′55.81″W) and Maelifellssandur (63°48′48.7″N 19°07′42.5″W). These regions and their properties have been described in detail elsewhere.[5] Briefly, they are subject to strong aeolian erosion due to frequent dust storms, and span large areas (10 to 140 km^2), hence providing a substantial supply of dust to the atmosphere.[5] Much of this dust is made of basaltic tephra and lava parent material that has been weathered by chemical and physical (*e.g.* glacio-fluvial) processes.[5] The samples were collected from the top centimeter of the surface, *i.e.*, the surface active layer composed of freshly deposited dust. Physical and chemical properties of the v-dusts have been previously characterized and are reported elsewhere.[24,26]

To further characterize the v-dust samples, we determined the surface (topmost 2–10 nm) elemental composition of the v-dusts by X-ray Photoelectron Spectroscopy (XPS) using a Kratos Axis Ultra Instrument. Relative concentrations (in at%) were determined by high-resolution scans at a pass energy of 40 eV for C_{1s}, O_{1s}, Si_{2p}, Al_{2p}, Fe_{2p}, Mg_{2p}, Ca_{2p}, Na_{1s}, K_{2p}, Ti_{2p}, and Mn_{2p} using a monochromatic Al X-ray beam centered at 1486.6 eV. Data treatment was performed using the CasaXPS software. The binding energy scale was calibrated by fixing the C_{1s} peak for adventitious carbon at 284.8 eV.[27] The results are presented in Table 1.

2.1.2. Gases. The kinetic measurements are carried out using zero air as bath gas, supplied by a Claind ZeroAir 2020 generator. In experiments requiring humid air, a second flow of zero air going through a bubbler of ultrapure water (Milli-Q, resistivity 18.2 MΩ cm) is mixed with the dry air flow in proportions necessary to reach the targeted RH value. The SO_2 gas cylinder is provided by Air Liquide, with $[SO_2] = 8.96$ ppm in air (20.7% O_2, 79.3% N_2). Dry air, humid air and SO_2 flows are controlled by MKS mass-flow controllers (100 to 1000 sccm, standard cubic centimeters per minute) connected to a four-channel MKS type 247 readout unit. The gases are pre-mixed in the gas lines before injection into the reactor.

2.2. Experimental setup

The heterogeneous interaction of SO_2 with the v-dust materials is studied in a horizontal coated-wall flow-tube (CWFT) reactor

Table 1 Surface composition, expressed in at%, of the v-dusts used in this study, excluding O and C

V-dust	Si	Al	Fe	Mg	Ca	Na	K	Ti	Mn
Mýrdalssandur	53.1	17.6	11.7	4.4	6.6	3.3	0.7	2.6	<0.1
Dyngjusandur	53.9	19.9	9.1	6.4	7.7	1.4	<0.1	1.4	0.3
Hagavatn	45.0	35.8	5.7	3.1	6.9	1.9	<0.1	1.1	0.1
Maelifellssandur	49.8	22.3	13.0	4.1	5.2	1.9	0.4	3.0	0.4

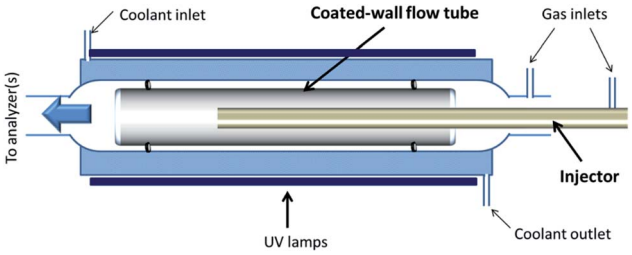

Fig. 1 Schematic representation of the coated-wall flow-tube (CWFT) reactor. The space filled with coolant between the two walls is shaded in blue. The dust sample coating the inner surface of the Pyrex tube is shown in gray.

at atmospheric pressure and room temperature $T = 296$ K (Fig. 1).[24,26,28] The v-dust sample is deposited on the inner surface of a Pyrex tube. Further details about the sample preparation can be found in recent publications.[24,26] The tube is then inserted into the reactor along its main axis, and kept in position by two Viton O-rings sealing the space between the tube and the wall of the reactor. Before each experiment, the sample is left for at least 1 hour under a zero air flow at the RH to be used during the subsequent experiment. This allows equilibration of the surface of the v-dusts with H_2O at the desired level of RH, prior to exposure to SO_2.

Air and SO_2 are flowed through a movable injector with an internal diameter of 0.3 cm. The total flow rate ranges from 250 to 500 sccm, ensuring laminar flow conditions (Reynolds number Re < 150). A thermoregulation unit (Huber, Ministat 230) controls the temperature by circulating water between the double-wall of the flow-tube. In separate experiments, the temperature profile of the gas flow along the reactor was recorded by inserting a K-type thermocouple into the movable injector; the temperature was found to be constant along the flow-tube and consistent with the value displayed by the thermoregulation unit (±1%).

Downstream of the reactor, the outgoing flow is directed to a SO_2 analyzer (Model 43C, Thermo Environmental Instruments Inc.), where SO_2 is detected *via* its fluorescence signal after absorption of UV photons. The limit of detection is 2.0 ppb for the average time of 10 seconds set in our experiments. The precision of the measurement given by the supplier of the instrument is 1.0 ppb or 1% of the reading, whichever is greater. Throughout this study, gas concentrations are given in ppb; under usual experimental conditions ($T = 296$ K, $P = 1$ atm), 1 ppb (SO_2) ≈ 2.5×10^{10} molecules cm^{-3}.

Three UVA lamps (UVA, Philips Lighting PL-L 18 W/10/4P; 315–400 nm with maximum emission at 352 nm) are placed evenly around the flow-tube at a distance of 12 cm in order to investigate possible photo-induced reactions on the surface of the v-dusts. The light source is characterized by measuring the photolysis rate of NO_2 in the reactor, J_{NO_2}. The J_{NO_2} values measured after switching on one, two or three UV lamps are 1.5×10^{-3} s^{-1}, 3.0×10^{-3} s^{-1} and 4.5×10^{-3} s^{-1}, respectively, similar to the J_{NO_2} measured in the Earth's atmosphere under cloudy and clear sky conditions.[29–31]

2.3.1. Experimental protocol. A theoretical SO_2 concentration [SO_2] profile is represented in Fig. 2. This profile describes the observed response of the SO_2 trace gas concentration as a function of the v-dust surface exposure time under dark and UV irradiation conditions. During a typical flow-tube experiment with v-dust, SO_2 is flowed through the reactor, the dust being left unexposed initially. After a stable initial SO_2 concentration, $[SO_2]_0$, is established, the injector is pulled out and the dust is exposed to SO_2 in the dark. The change in [SO_2] related to gas uptake by the dust is recorded by the SO_2 analyzer downstream of the reactor. Once a steady-state is reached in the dark, $[SO_2]_{ss,dark}$, the UV lamps are turned on and [SO_2] is recorded. The lamps are turned off after a new steady-state concentration of SO_2 is reached, $[SO_2]_{ss,light}$, and the injector is pushed back in the reactor to return to the initial $[SO_2]_0$. The so-called SO_2 "breakthrough curve" is used to determine the steady-state SO_2 uptake coefficients.[32] As described in Urupina *et al.*,[24] a long-lasting tail is observed on the breakthrough curve in the case of SO_2 interacting with v-dust, similar to that observed during the interaction of nitric acid (HNO_3) with ice.[32] This raises the question of the moment at which it can be assumed that a steady-state is reached. We adopt a pragmatic definition as given in our recent paper:[24] a steady-state is considered to be reached when the variation of the signal is smaller than 1 ppb for at least one hour.[24] In the case of SO_2 uptake by v-dust at 30% RH (Fig. 2), it takes about 6–12 hours to reach a steady-state in the dark and 20–36 hours under UV irradiation. These temporal milestones are used as a point of comparison between the different v-dust samples. Fig. S1† displays typical uptake profiles of SO_2 recorded at 10% and 50% RH. To determine [SO_2] at steady-state in the dark and under UV irradiation in systems requiring a very long time to reach equilibrium, the breakthrough curve is fitted with an exponential function to obtain an extrapolated value of [SO_2] at $t = \infty$, which is used to calculate the steady-state uptake coefficient.

2.3.2. Determination of the initial number of SO_2 molecules taken up. The initial number of SO_2 molecules taken up per unit of surface of the v-dusts, N_S (molecules cm^{-2}), is determined by integrating the area above the breakthrough curves (Fig. 2), divided by the effective surface area of the dust, A_s, according to (1):

$$N_s = \int_{t=\text{exposure}}^{t=\text{steady-state}} \frac{F}{A_s} \mathrm{d}t \quad (1)$$

where $F(t)$ is the flow rate (SO_2 molecules min^{-1}) through the reactor. Note that exposure of a clean flow-tube to SO_2 (in the absence of v-dust) under both dark and light conditions evidenced a negligible loss of SO_2 gas. Thus, the possible uptake of SO_2 by solvation in layers of water molecules adsorbed at the air–solid interface is unlikely under our experimental conditions.[33]

Since the SO_2 concentrations recorded at steady-state both in the dark and under UV irradiation are lower than pre-exposure concentrations, only the initial removal of SO_2 is considered (dashed areas in Fig. 2) in the determination of N_S. The integration limits for the determination of N_S correspond to the

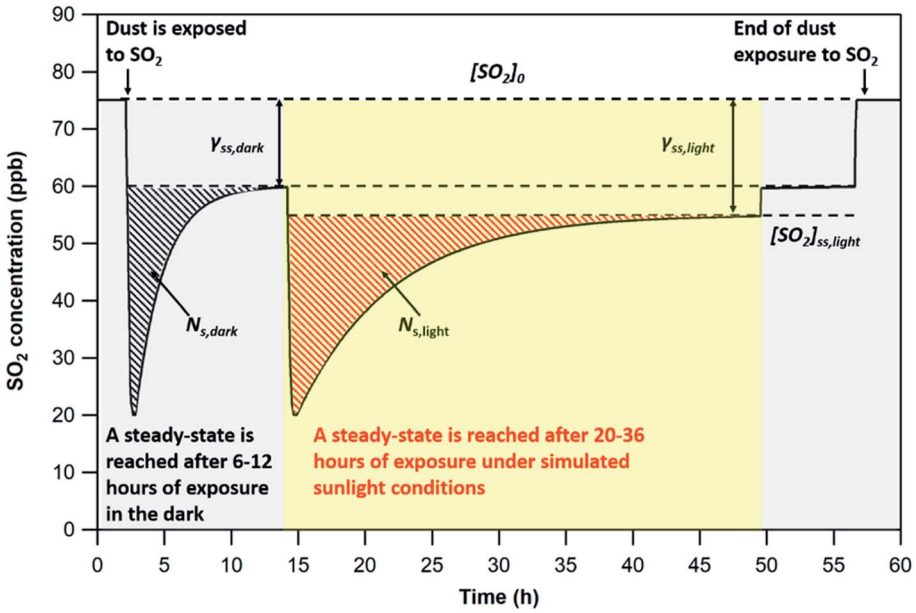

Fig. 2 Theoretical SO_2 concentration profile during a typical flow-tube experiment with v-dust at 296 K. At the beginning of the experiment, the dust is isolated from the gas mixture, in which an initial SO_2 concentration, $[SO_2]_0$, is set. The dust is then exposed to SO_2 in the dark (gray area), and $[SO_2]$ decreases initially strongly, before recovering to a steady-state value $[SO_2]_{SS,dark}$ within typically 6–12 hours. Thereafter, the surface is irradiated with UV light (yellow area), and a second large consumption of SO_2 is observed, before recovering to a steady-state value $[SO_2]_{SS,light}$ within typically 20–36 hours. Lights are turned off (second gray area) and $[SO_2]$ returns to its steady-state value in the dark. The SO_2 concentration is then returned to $[SO_2]_0$ by pushing the injector in, and the dust is no longer exposed to the gas. Black-shaded and red-shaded areas correspond to the initial number of SO_2 molecules taken up per surface unit of v-dust (in molecules cm^{-2}), respectively in the dark and under UV, $N_{S,dark}$ and $N_{S,light}$. The moment at which the steady-state is reached (as discussed earlier, see text) is chosen as integration limit for the determination of N_S. $[SO_2]_{SS,dark}$ and $[SO_2]_{SS,light}$ are used to measure the steady-state uptake coefficients, $\gamma_{ss,dark}$ and $\gamma_{ss,light}$.

period of time elapsed between exposure of the dust to SO_2 and steady-state (*i.e.*, maximum signal variation of 1.5% for at least three hours). This criterion is adopted to compare the uptake capacities of the four v-dusts at the initial stage of interaction with SO_2.

2.3.3. Determination of the steady-state uptake coefficients. The uptake coefficient of SO_2 on the surface of the v-dust material is derived using eqn (2):

$$\gamma_{geom} = \frac{2 \times k_{kin} \times r_{tube}}{C_{SO_2}} \quad (2)$$

where γ_{geom} is the geometric uptake coefficient, k_{kin} (s^{-1}) is the first order rate coefficient of heterogeneous SO_2 loss in the kinetic regime (the regime where diffusion corrections are negligible), r_{tube} (cm) is the radius of the tube, and C_{SO2} (cm s^{-1}) is the average molecular velocity. The radius of the tube (0.49 cm) and the average molecular speed of SO_2 at 296 K are known, thus only k_{kin} needs to be determined. The experimental validation of first order kinetics of k_{kin} is provided in Fig. S2.† Details on the calculation of the uptake coefficients and diffusion corrections, the latter were always below 7%, are provided elsewhere.[26,34–36]

The uptake coefficient determined using the geometric surface area (S_{geom}) of dust can be considered an upper limit.[20] A more realistic estimate of the surface area probed by gas molecules is made using the Brunauer, Emmett and Teller specific surface area, S_{BET} (m^2 g^{-1}), of the solid sample.[37] The BET surface areas of the v-dusts studied here are presented in Table S1.† The effective surface area of the v-dust is then given by $A_s = m_{dust} \times S_{BET}$, where m_{dust} is the mass of dust deposited on the walls of the flow-tube. The corresponding uptake coefficient (γ_{BET}) is given by the following expression:

$$\gamma_{BET} = \frac{\gamma_{geom} \times S_{geom}}{A_s} \quad (3)$$

In order to investigate whether the entire v-dust surface is accessible to SO_2 or not, k_{kin} was determined under steady-state conditions in a series of experiments where different v-dust masses were exposed to SO_2. The results obtained for Mýrdalssandur v-dust are displayed in Fig. 3. For comparison purpose, k_{kin} calculated for a clean tube is also presented. While a negligible adsorption of SO_2 occurs on a clean tube, the precision of the SO_2 analyser (*i.e.*, 1 ppb) enables determination of the value of k_{kin} in a clean tube. The results shown in Fig. 3 were fitted with a linear function that excludes the datapoint estimated for a clean tube. Note that k_{kin} increases linearly with the mass of dust, which indicates that the entire surface of dust is accessible to SO_2 gas and participates in the heterogeneous loss of SO_2. The linear fit intersects (within error) the k_{kin} value estimated for a clean tube, confirming the robustness of our measurements. In the following, experiments are performed with v-dust masses in the linear regime and adjusting the flow rate to lower values to increase the precision of the k_{kin} values measured under steady-state conditions.

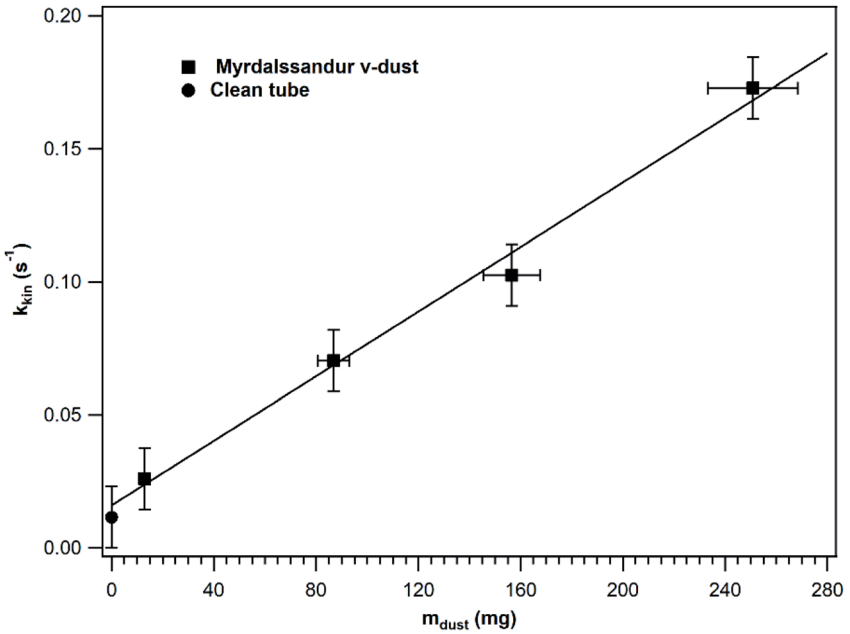

Fig. 3 k_{kin} values (in s^{-1}) measured under steady-state conditions as a function of the mass of Mýrdalssandur v-dust deposited (squares). The experiments were performed at 296 K under dry and dark conditions, with $[SO_2]$ fixed at 75 ppb. For comparison, the k_{kin} value estimated on a clean tube is also presented (circle). The solid line is the linear fit of the experimental results (excluding the value estimated for a clean tube). The error on the values of k_{kin} corresponds to the precision of the measurement and includes estimated uncertainties. The error bars on m_{dust} reflect the uncertainties on the mass of v-dust deposited, and mainly originate from the mass lost (<7%) during the experiment, as measured before and after the experiment.

2.3.4. Error analysis. To calculate the uncertainty on N_S, we include the 2σ standard deviation of the integrated area of the adsorption peaks (*ca.* 7%), the errors on the gas flow measurement, temperature, mass weight, and length of the exposed dust coating (accounting for ~8%), and the uncertainty on S_{BET} (~25%). The total absolute uncertainty on N_S is calculated by adding the individual uncertainties in quadrature, and is estimated to be ~30%. In several instances, to evaluate the effect of photo-irradiation on N_S values determined under various atmospheric conditions or with different samples, we define the amplification factor, $N_{S,light}/N_{S,dark}$. In this case, based on eqn (1), the ratio $N_{S,light}/N_{S,dark}$ calculated for a single type of dust makes A_s terms cancel out, hence the relative uncertainty on N_S decreases to about 10%. This approach using the ratio $N_{S,light}/N_{S,dark}$ aims to evaluate the impact of irradiation on each other experimental parameter modified, as described in the Results section.

Regarding the steady-state uptake coefficient, considering the precision of the signal (1 ppb) and its propagation to k_{obs}, the determination of S_{BET} and all relevant uncertainties on the gas flow measurement, temperature, mass weight, and length of the exposed dust coating, the overall uncertainty is ~8%. The total error calculated for the γ values is estimated to be ~35%, and mainly stems from the precision of the SO_2 concentration measured at steady-state and after isolation of the surface. In all experiments, a conservative limit of 40% uncertainty in $\gamma_{SS,BET}$ is given.

3. Results and discussion

3.1. Initial number of SO_2 molecules taken up on v-dust samples

3.1.1. Impact of surface elemental composition on N_S values. The initial number of molecules taken up by v-dusts, N_S, is measured at RH = 30%, T = 296 K and $[SO_2]_0$ = 75 ppb, both in the dark and under UV light ($J_{NO_2} = 4.5 \times 10^{-3}$ s^{-1}). The $N_{S,dark}$ and $N_{S,light}$ values range from 10^{13} to 10^{14} molecules cm^{-2} (Table 2).

Under dark conditions, N_S values determined for the different v-dust samples range from 0.96 to 2.5 $\times$ 10^{13} molecules cm^{-2}. The variation observed may be attributed to differences in the physical (*e.g.*, morphology, crystallinity,

Table 2 Initial number of SO_2 molecules taken up, N_S, measured on the v-dusts in the dark and under UV light ($J_{NO_2} = 4.5 \times 10^{-3}$ s^{-1}) under controlled experimental conditions: $[SO_2]_0$ = 75 ppb, RH = 30% and T = 296 K

	Initial number of SO_2 molecules taken up, N_S (in 10^{13} molecules cm^{-2})		
V-dust	$N_{S,dark}$	$N_{S,light}$	$N_{S,light}/N_{S,dark}$
Mýrdalssandur	3.0 ± 0.9	9.3 ± 3.0	3.1 ± 0.31
Dyngjusandur	2.1 ± 0.6	3.6 ± 1.0	1.7 ± 0.17
Hagavatn	1.2 ± 0.4	2.0 ± 0.6	1.7 ± 0.17
Maelifellssandur	0.96 ± 0.29	3.7 ± 1.1	4.0 ± 0.40

hygroscopicity) and/or chemical (*e.g.*, surface elemental composition) properties of the particles. A schematic representation of the general reaction mechanism of SO_2 at the surface of v-dust reported in a previous study[24] is given below:

$$SO_{2(gas)} + SS \overset{H_2O}{\leftrightarrow} SS - SO_{2(ads)} \quad (R1)$$

$$SS - SO_{2(ads)} \overset{H_2O}{\longrightarrow} SS - {SO_3}^{2-}{}_{(ads)} \text{ or } SS - {HSO_3}^{-}{}_{(ads)} \quad (R2)$$

$$SS - {SO_3}^{2-}{}_{(ads)} \text{ or } SS - {HSO_3}^{-}{}_{(ads)} \overset{H_2O}{\longrightarrow} SS - {SO_4}^{2-}{}_{(ads)} \text{ or } SS - {HSO_4}^{-}{}_{(ads)} \quad (R3)$$

where SS represents a surface site, SS–${SO_3}^{2-}{}_{(ads)}$ and SS–${HSO_3}^{-}{}_{(ads)}$ are adsorbed sulfite (${SO_3}^{2-}$) and bisulfite (${HSO_3}^{-}$), and SS–${SO_4}^{2-}{}_{(ads)}$ and SS–${HSO_4}^{-}{}_{(ads)}$ are adsorbed sulfate (${SO_4}^{2-}$) and bisulfate (${HSO_4}^{-}$); they are the final products of the surface reaction process.

Under UV irradiation, N_S increases by a factor ranging from 1.7 to 3.8 relative to dark conditions, depending on the type of v-dust. The enhanced removal of SO_2 in the presence of UV photons may be attributed to photo-induced processes occurring at the v-dust/air interface. In our experiments, we cannot discriminate photon activation of v-dust from photon activation of surface groups or of adsorbed species. Therefore, several points are useful to highlight in considering the nature of this photo-induction:

(i) It is well established that reactive species (*i.e.*, hydroxyl radicals, $^{\bullet}OH$, hydroperoxyl radicals, $^{\bullet}O_2H$, or superoxide radicals, $O_2^{\bullet-}$, *etc.*) form on the surface of mineral dusts containing Ti and Fe under UV/visible light irradiation in the presence of H_2O.[38–40] Therefore, these reactive species likely formed on the surface of v-dust, contributing to SO_2 uptake.

(ii) Under our experimental conditions, no photolysis of SO_2 has been observed, since it requires photons with wavelengths lower than 220 nm,[33] which are absent from the emission spectrum of our lamps. Direct photochemistry of ${SO_4}^{2-}$ species does not occur either, since ${SO_4}^{2-}$ does not absorb photons between 310 and 400 nm.[41]

(iii) Although the absorption of photons by ${SO_3}^{2-}$ in the 310–410 nm range remains very low, it cannot be neglected. Thus, irradiation of v-dust may lead to ${SO_3}^{2-}$ surface photochemistry, forming low amounts of $^{\bullet}{SO_3}^{-}{}_{(ads)}$,[42] which in turn, can lead to H_2SO_4 formation in the presence of H_2O.[43]

Thus, irradiation of the surface of v-dust may create new active surface sites that promote SO_2 uptake (reaction (R1)) and/or provide new reactive pathways enhancing the oxidation of intermediate species in the mechanism of SO_2 transformation (reactions (R2) and (R3)). However, monitoring only the gas phase, as we do in these experiments, does not enable assessment of the contribution of each process to the overall consumption of SO_2 gas.

In an attempt to evaluate further the observed trends, we investigate whether the amplification factor, $N_{S,light}/N_{S,dark}$ is correlated with the surface elemental composition of the v-dust samples. It is well established that mineral oxides containing Ti are photoactivated under UV-A light irradiation, and create reactive surface species.[38–40,44] Iron-bearing minerals are also photoactive, but mainly under visible light. In this context, we display in Fig. 4 the $N_{S,light}/N_{S,dark}$ ratio plotted as a function of the surface Ti concentration (Fig. 4a), and of the surface Ti/Si ratio (Fig. 4b). We observe a linear increase of $N_{S,light}/N_{S,dark}$ with both surface Ti and Ti/Si. Trends observed with elemental Fe are not straightforward, and are therefore not discussed. We propose that the photo-enhanced uptake of SO_2 is related to the presence of Ti at the surface of v-dust. To parametrize these results (see also Section 3.1.4.), we choose the surface Ti content relative to the most abundant element in v-dust (*i.e.* the surface Ti/Si ratio) to facilitate comparison across samples of different composition. Therefore, based on Fig. 4b, we propose an empirical parametrization of the amplification factor (4) relevant under our experimental conditions and for the v-dust samples studied:

$$N_{S,light}/N_{S,dark} = 65.1 \times (Ti/Si) \quad (4)$$

The dependence of the amplification factor on surface Ti/Si content suggests that active surface species (*e.g.* $^{\bullet}OH$, $^{\bullet}O_2H$, $O_2^{\bullet-}$) may be formed on the surface of v-dust (point (i) above), enhancing SO_2 consumption. Nevertheless, considering the uptake profiles in Fig. S1† (and illustrated in Fig. 2), and the

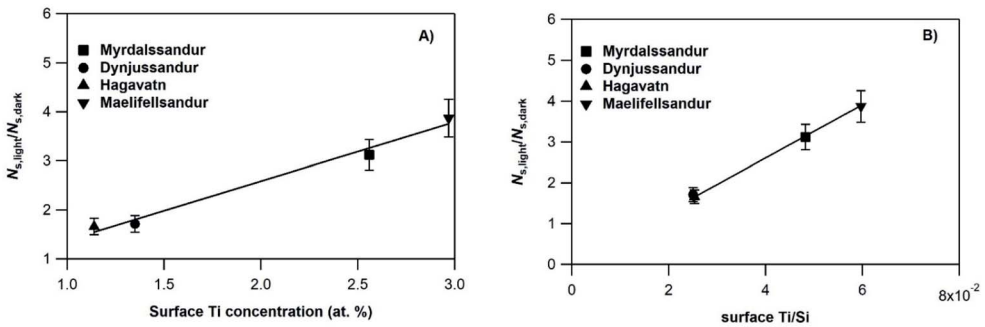

Fig. 4 Amplification by light of the initial number of SO_2 molecules taken up on the v-dust samples, $N_{S,light}/N_{S,dark}$, as a function of: (A) surface Ti concentration, and (B) surface Ti/Si concentration ratio, as measured by XPS. The experimental conditions were: $[SO_2]_0 = 75$ ppb, RH = 30% and $T = 296$ K, in the dark, and $J_{NO_2} = 4.5 \times 10^{-3}$ s^{-1} during UV irradiation experiments. The solid lines show linear fits of the experimental results, with a correlation coefficient $R^2 > 0.97$ for Ti surface concentration and $R^2 > 0.99$ for the Ti/Si ratio.

gradual saturation/deactivation of the surface with time, the process cannot be characterized as catalytic. In addition, other photo-induced processes, such as photolysis of surface intermediate species (*e.g.* SO_3^{2-}; point (iii) above), should not be discarded.

In subsequent experiments to evaluate the impact of other relevant atmospheric parameters (photon flux and RH) on the photo-promoted removal of SO_2, we choose Mýrdalssandur v-dust as a model sample. The major criterion for this selection is the high uptake capacity (high N_S values) of the sample under both dark and UV light conditions, coupled with a large amplification factor under light with respect to dark conditions (see Table 2).

3.1.2. Dependence of N_S on photon flux. To evaluate the impact of light intensity on the uptake of SO_2 by Mýrdalssandur v-dust, a series of experiments are performed at 30% RH, 296 K and 75 ppb of SO_2, varying the UV photon flux ($J_{NO_2} = 0$–4.5×10^{-3} s^{-1}). The results are presented in Fig. 5, where $N_{S,light}/N_{S,dark}$ is plotted as a function of J_{NO_2}. $N_{S,light}/N_{S,dark}$ increases linearly with the photon flux, indicating that the consumption of SO_2 molecules from the gas phase is proportional to the photon flux irradiating the surface.[38] An amplification of N_S by a factor of three compared to dark conditions is observed for the highest irradiance ($J_{NO_2} = 4.5 \times 10^{-3}$ s^{-1}). The linear increase of N_S with UV light intensity confirms that the number of photons illuminating the surface does not saturate the photo-process, leading to an enhanced consumption of SO_2. Since the objective of this work is to investigate the photo-enhanced removal of SO_2 under relevant atmospheric conditions using realistic photon fluxes, higher light intensities are not explored. The linear correlation of N_S with light intensity can be attributed to photo-induced processes on the surface leading to SO_2 consumption.

Photo-induced removal of atmospheric species has been highlighted in previous studies dealing with the degradation of pollutants on the surface of mineral dust proxies,[34,45,46] and on v-dusts,[26] but an accurate description of the heterogeneous physicochemical pathway involved is still lacking. The nature of the photo-induced surface processes can involve complementary surface sites activated by light, or alternatively photo-enhanced surface reactions promoting the transformation of SO_2 into surface species such as SO_3^{2-}/HSO_3^- or SO_4^{2-}/HSO_4^- (reactions (R1)–(R3)).

In all cases, based on the breakthrough profiles recorded under different irradiation intensities, a gradual recovery of SO_2 concentration with time is observed (see Fig. 2). In spite of the enhancement brought by UV light, SO_2 uptake remains a transient process, attesting to the aging of the surface and its deactivation irrespective of the magnitude of the photon enhancement observed here.

Eqn (5) is proposed as an empirical description of the photo-enhanced consumption of SO_2 under the current experimental conditions:

$$N_{s,light}/N_{s,dark} = 1 + 480.5 \times J_{NO2} \quad (5)$$

3.1.3. Dependence of N_S on RH. Relative humidity is an important atmospheric parameter that can influence the uptake of pollutants on the surface of mineral dusts and other airborne solid particles. Water molecules can (i) block active sites, hindering the uptake of gases;[47,48] (ii) form water layers at the surface of particles, thus promoting the formation of reaction products;[24,49] (iii) provide radical species, especially under light irradiation, thereby promoting reactive processes.[38–40,50,51] Joshi *et al.*[52] investigated the adsorption isotherms of H_2O on Icelandic volcanic ash. They observed a BET-type adsorption isotherm, with a rapid increase of surface water concentration from 0 to 20–30% RH, when the water monolayer is completed. Above the monolayer threshold, the surface water content increases linearly up to *ca.* 72% RH. At higher RH an exponential increase is reported. These results suggest that under the humid conditions explored in our study (from 10 to 72% RH), the surface coverage of v-dusts by water molecules tends to correlate linearly with RH.

To evaluate the impact of RH on the uptake of SO_2, we exposed Mýrdalssandur v-dust to a fixed concentration of SO_2 under both dark conditions and UV irradiation ($J_{NO_2} = 4.5 \times 10^{-3}$ s^{-1}) at 296 K, and varying RH in the 0.1–72% range. The results are presented in Table 3. $N_{S,dark}$ increases from 0.1 to 30% RH before reaching a saturation regime and remaining almost constant. This observation points to a two-fold role played by water molecules in the removal of SO_2. As RH increases from 0.1 to 30%, the consumption of SO_2 is enhanced by the formation of OH groups on the surface of v-dust. Surface OH groups assist the transformation of SO_2 to surface SO_3^- and SO_4^{2-} species, as evidenced by Urupina *et al.*[24] Above 30% RH, *i.e.*, beyond the water monolayer formation on dust,[52,53] we suggest a competition between two processes: the formation of OH groups promoting the removal of SO_2, and the blocking of active surface sites by molecularly adsorbed water. The

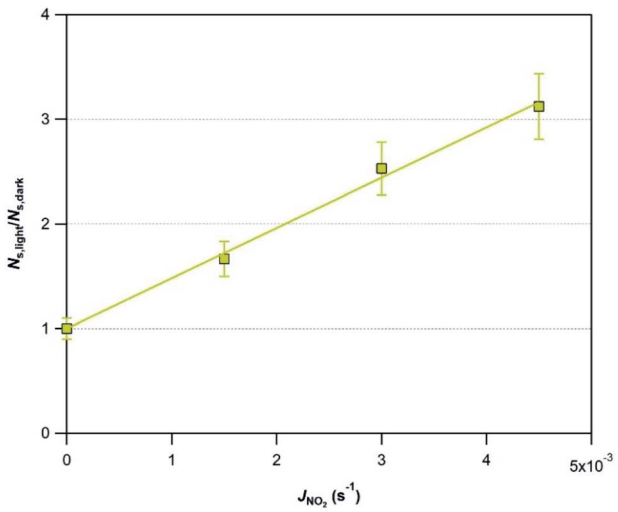

Fig. 5 Amplification by light of the initial number of SO_2 molecules taken up on Mýrdalssandur v-dust, $N_{S,light}/N_{S,dark}$, as a function of the photon flux ($J_{NO_2} = 0$–4.5×10^{-3} s^{-1}). Mýrdalssandur v-dust was exposed to 75 ppb of SO_2 at RH = 30% and $T = 296$ K.

Table 3 Initial number of SO_2 molecules taken up in the dark, $N_{S,dark}$, and under UV light ($J_{NO_2} = 4.5 \times 10^{-3}$ s^{-1}), $N_{S,light}$, as a function of RH for Mýrdalssandur v-dust exposed to 75 ppb of SO_2 at $T = 296$ K

	Initial number of SO_2 molecules taken up, N_S (in 10^{13} molecules cm^{-2})		
RH (%)	$N_{S,dark}$	$N_{S,light}$	$N_{S,light}/N_{S,dark}$
0.1	0.39 ± 0.12	—	—
10	2.3 ± 0.7	4.0 ± 1.2	1.7 ± 0.2
30	3.0 ± 0.9	9.5 ± 2.8	3.2 ± 0.3
50	3.3 ± 1.0	17 ± 5.0	5.2 ± 0.5
72	3.6 ± 1.1	23 ± 7.0	6.4 ± 0.6

antagonistic nature of the two processes may account for the saturation of $N_{S,dark}$.

In contrast, when the surface is irradiated, $N_{S,light}$ increases over the whole range of RH values and saturation does not occur. The blank experiments (in the absence of dust), carried out under UV light, evidence a negligible removal of SO_2 at RH = 30%. During these experiments, multilayers of water molecules are formed on the walls of the flow-tube reactor. The absence of any contribution from water-covered surfaces to SO_2 uptake indicates that solvation reactions at the adsorbed water/air interface are negligible. The linear increase of $N_{S,light}$ with RH cannot be directly attributed to RH, but to photo-induced processes. These processes may be related to Ti-surface sites activation, leading to the formation of reactive surface species,[38,39] or to surface photochemistry involving adsorbed species and promoting the oxidation mechanism of SO_2.[40,54,55] These observations support the hypothesis made in Section 3.1.1.; the increase of SO_2 removal observed under light for various values of RH is due to the generation of new surface sites and/or to the activation of new reaction pathways promoting the transformation of SO_2 or of intermediate species to final products (reactions (R1)–(R3)).

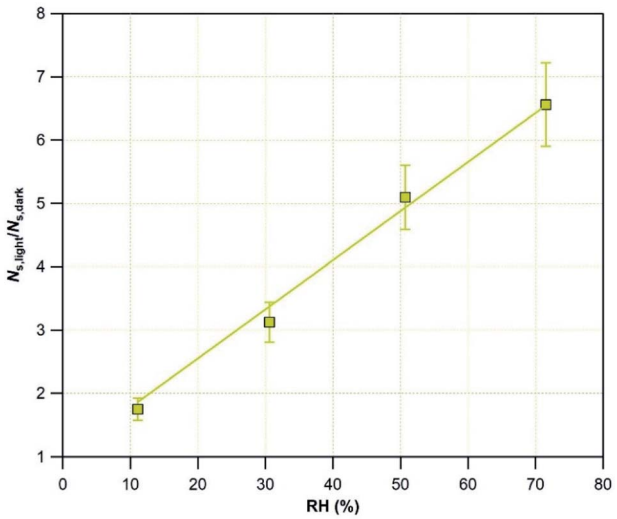

Fig. 6 The amplification factor, $N_{S,light}/N_{S,dark}$, plotted as a function of RH for Mýrdalssandur v-dust exposed to 75 ppb of SO_2 at $T = 296$ K. The yellow line is the linear fit of the results.

To quantify the enhancement of N_S in the presence of light, in Fig. 6 the amplification factor is plotted as a function of RH. The results are linearly fitted with eqn (6):

$$N_{S,light}/N_{S,dark} = 1 + (7.76 \times 10^{-2}) \times RH \quad (6)$$

3.1.4. Global parametrization of N_S. Our experimental observations evidence a photo-enhanced uptake of SO_2 on natural v-dust samples. The key factors driving the photo-enhanced uptake of SO_2 by v-dust are: (i) surface composition, (ii) light intensity, and (iii) RH. The mechanism of gas-phase SO_2 removal may be attributed to the photo-activation of additional surface sites, and/or to the photo-enhancement of the reactivity of specific adsorbed intermediate species in a sequence of consecutive reactions leading to the final products (reactions (R1)–(R3)).

Based on the experimental approach followed, including (i) screening the v-dusts to assess their capacity for SO_2 uptake and (ii) tuning individual atmospheric parameters (UV light irradiation and RH) and evaluating their impacts on SO_2 removal, the experimental results for Mýrdalssandur v-dust are parametrized with eqn (4)–(6). We propose a general eqn (7) describing the correlation between the amplification factor with the chemical composition of the sample, the photon flux, and RH:

$$N_{S,light}/N_{S,dark} = 6.1 \times (1 + 7.76 \times 10^{-2} \times RH) \times (1 + 480.5 \times J_{NO2}) \times (Ti/Si) \quad (7)$$

Despite the fact that we did not perform a detailed RH dependence for all types of v-dusts, eqn (7) succeeds in describing the expected amplification factors for the other samples within 10% uncertainty. This type of empirical equation is useful in modeling because relevant atmospheric parameters are gathered to give a global description of the photo-enhanced removal of SO_2. It should be stressed that the proposed parametrization concerns the results of the current study performed under specific experimental conditions of RH and photon flux, using a limited range of v-dust compositions, and requires validation with a more experimental conditions and samples before a general application can be recommended.

3.1.5. Comparison with the literature. To the best of our knowledge, the present work is the first to report the long-lasting aging of natural v-dust particles by SO_2 under UV irradiation. It is therefore difficult to compare directly the results determined in the current study with those reported in the literature, since the substrates studied, and the experimental conditions and timescales, differ. Nevertheless, we compare the results obtained in this work with those reported for natural dust and volcanic ash samples below.

The values of $N_{S,dark}$ measured in our study range between 1 and 3 × 10^{13} molecules cm^{-2} at RH = 30%. They are in good agreement with Maters *et al.*,[23] who report values of $N_{S,dark}$ in the 10^{11}–10^{13} molecules cm^{-2} range for SO_2 uptake by volcanic ash and glass powders. Our values are also close to those measured on Saharan dusts at 27% RH, but on a much shorter

timescale and under different experimental conditions (pressure, absence of oxygen, *etc.*).[56]

Sulfur dioxide removed from the gas phase is expected to be converted into SO_3^{2-} and SO_4^{2-} species. Under dark conditions, several authors have reported different pathways of SO_2 transformation (see Urupina *et al.*[24] and references therein). Under UV light, the transformation of SO_2 has been studied in a simulation chamber on airborne Arizona Test Dust (ATD) particles. Nevertheless, these experiments were carried out in the presence of NO_x and O_3, generating $^{\bullet}OH$ radicals in the gas phase, which further oxidize SO_2 to SO_4^{2-}. Even in the set of experiments carried out in the absence of NO_x, $^{\bullet}OH$ radicals were always present (due to outgassing of NO_x and NO_y from the wall of the reactor).[57,58] Therefore, no direct comparison to our data can be made.

3.2. Steady-state uptake of SO_2 on v-dust samples

3.2.1. Effect of UV light irradiation on $\gamma_{SS,BET}$. After quantifying the initial SO_2 uptake, $N_{S,dark}$ and $N_{S,light}$, we now turn to the determination of the steady-state uptake coefficients, $\gamma_{SS,BET}$. Sulfur dioxide uptake by the four Icelandic v-dusts is studied at RH = 30%, T = 296 K and $[SO_2]_0$ = 75 ppb, in the dark and under UV irradiation ($J_{NO2} = 4.5 \times 10^{-3}$ s^{-1}). The $\gamma_{SS,BET}$ values fall in the 10^{-8} to 10^{-7} range under UV irradiation, and in the 10^{-9} to 10^{-8} range in the dark (Table 4). Under dark conditions, the most reactive sample towards SO_2 is Mýrdalssandur v-dust, displaying the highest $\gamma_{SS,BET}$ and N_S values among the v-dusts tested. Under UV irradiation, Mýrdalssandur v-dust is still among the most reactive samples. Meanwhile, the amplification factor of $\gamma_{SS,BET}$, $\gamma_{SS,BET,light}/\gamma_{SS,BET,dark}$, is the lowest among the four v-dusts tested (Table 4).

All v-dust samples exhibit a photo-enhanced uptake of SO_2 under initial and steady-state regimes; they are nonetheless characterized by contrasted amplification factors. Interestingly, Mýrdalssandur and Maelifellssandur samples have high $N_{S,light}/N_{S,dark}$ ratios, but exhibit the lowest $\gamma_{SS,BET,light}/\gamma_{SS,BET,dark}$ ratios, whereas Hagavatn and Dyngjusandur samples exhibit lower $N_{S,light}/N_{S,dark}$ values, but higher $\gamma_{SS,BET,light}/\gamma_{SS,BET,dark}$ values. For Mýrdalssandur and Maelifellssandur samples, the number and/or the reactivity of the surface sites at the beginning of UV irradiation is significantly higher than for Dyngjusandur and Hagavatn, leading to an important light-induced consumption of gas-phase SO_2, as reflected by the values of $N_{S,light}/N_{S,dark}$ (Table 2). This is consistent with Mýrdalssandur and Maelifellssandur samples having the highest surface Ti/Si ratios (Table 1). However, the surface sites of Mýrdalssandur and Maelifellssandur dusts appear to be deactivated/exhausted faster than on the less reactive Dyngjusandur and Hagavatn samples, probably due to higher concentrations of surface products on the former materials, leading to lower $\gamma_{SS,BET,light}/\gamma_{SS,BET,dark}$ values. Considering the inverse correlation between initial and steady-state amplification factors, we suggest that the larger the number of surface sites involved in initial uptake, the lower the magnitude of the steady-state uptake coefficient. The initial uptake, which corresponds to N_S, seems to act as an ageing process on surface reactivity, hence lowering the uptake process at steady-state, characterized by $\gamma_{SS,BET}$.

Mýrdalssandur v-dust was used as a model sample to further evaluate the impact of atmospheric conditions on $\gamma_{SS,BET}$ (see Section 3.1.1.). Considering the relatively low increase in $\gamma_{SS,BET}$ after irradiation of the v-dust surface with the highest photon flux (*i.e.*, $J_{NO_2} = 4.5 \times 10^{-3}$ s^{-1}), experiments were not performed with lower J_{NO_2}. However, additional experiments were conducted to determine the uptake coefficients as a function of RH under dark and light irradiation ($J_{NO_2} = 4.5 \times 10^{-3}$ s^{-1}).

3.2.2. Dependence of $\gamma_{SS,BET,dark}$ and $\gamma_{SS,BET,light}$ on RH for Mýrdalssandur v-dust. To investigate the influence of RH on the steady-state uptake of SO_2 by Mýrdalssandur v-dust, experiments were conducted at 296 K, with $[SO_2]_0$ = 75 ppb, varying RH between 0.1 and 72%. The results obtained both under dark conditions and UV irradiation ($J_{NO2} = 4.5 \times 10^{-3}$ s^{-1}) are displayed in Fig. 7.

An increase of $\gamma_{SS,BET}$ by Mýrdalssandur v-dust is observed as RH increases from 0.1 to 30%. We suggest that this variation is related to the formation of a water monolayer at the surface of Mýrdalssandur v-dust. As reported by Urupina *et al.*,[24] the increase of the surface water content promotes the

Table 4 Steady-state BET uptake coefficients of the v-dusts measured in the dark and in the presence of UV light ($J_{NO_2} = 4.5 \times 10^{-3}$ s^{-1}) at $[SO_2]_0$ = 75 ppb, RH = 30% and T = 296 K

	Steady-state uptake coefficients, $\gamma_{SS,BET}$ (10^{-8})		
V-dust	$\gamma_{SS,BET,dark}$	$\gamma_{SS,BET,light}$	$\gamma_{SS,BET,light}/\gamma_{SS,BET,dark}$
Mýrdalssandur	6.2 ± 2.5	7.1 ± 2.9	1.1
Dyngjusandur	1.6 ± 0.6	7.3 ± 2.9	4.6
Hagavatn	0.66 ± 0.26	2.6 ± 1.0	3.9
Maelifellssandur	3.2 ± 1.3	6.6 ± 2.7	2.1

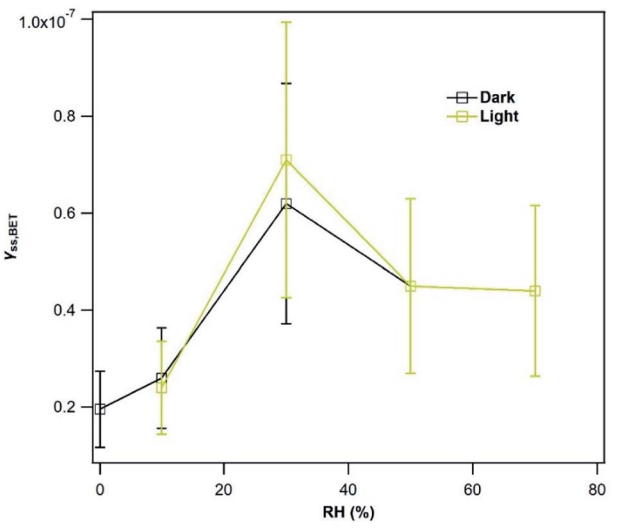

Fig. 7 Steady-state BET uptake coefficient, $\gamma_{SS,BET}$, as a function of RH during exposure of Mýrdalssandur v-dust to 75 ppb of SO_2 in the dark (black squares) and in the presence of UV light ($J_{NO_2} = 4.5 \times 10^{-3}$ s^{-1}; yellow squares) at T = 296 K. Datapoints in the dark at 50% and 70% RH overlap with those under light.

transformation of SO_2 into intermediate and final products (reactions (R1)–(R3)), and enhances the uptake of SO_2. The small reduction of the uptake coefficient as RH increases from 30 to 50% could be due to changes in the equilibrium by two effects: the enhanced removal/transformation of SO_2 on hydroxylated surface sites, and the competition of SO_2 with H_2O molecules for the same adsorption sites. Above 50%, the uptake coefficient seems to stabilize and become independent of RH. Nevertheless, we do not know what would be the behavior of SO_2 uptake for RH greater than 72%, where an exponential increase in the surface water concentration is anticipated based on the adsorption isotherms reported by Joshi *et al.*[52] Under UV light, despite the increasing initial consumption of SO_2 discussed previously, the formation of low-volatility final surface products deactivates the surface, and after 36 hours of exposure to light, $\gamma_{SS,BET,light}$ values are similar to those recorded in the dark.

3.2.3. Comparison with the literature. Dupart has studied the interaction of SO_2 with Eyjafjallajökull volcanic ash under UV irradiation.[59] At a SO_2 concentration of 190 ppb, and RH = 40%, the uptake of SO_2 is observed on a short timescale (~3 h) in the dark, and even shorter (~1.5 h) under UV light. In our experience, these timescales are not sufficient to reach a steady-state SO_2 uptake on v-dust, hence our experiments are much longer. The work of Dupart[59] shows: (i) a linear increase in the SO_2 uptake coefficient in the 10^{-7} range with the photon flux received by the surface of the volcanic ash; and (ii), an increase in the SO_2 uptake coefficient with RH between 15% and 40%, followed by a decrease up to roughly 50% RH. The behavior described in (ii) is consistent with our observations. We have not made experiments at RH = 40%, thus a further increase in SO_2 uptake between 30% and 40% RH is possible, although it cannot be seen in our results. We note however that the SO_2 uptake coefficients measured by Dupart are an order of magnitude higher than ours. This may be due to the different samples used (Eyjafjallajökull volcanic ash *versus* Icelandic v-dust) or to the fact that, under UV irradiation, the timescale of the SO_2 uptake measurement in Dupart's experiments is very short and might not be sufficient to reach a steady-state. This would lead to higher values of γ which do not truly reflect the steady-state uptake of SO_2.

The variations in the SO_2 uptake coefficient on the v-dusts with RH are qualitatively similar to those reported for two types of Chinese mineral dust, although the authors of these works observe a change in uptake above RH = 40%.[21] The difference in behavior with respect to RH may be due to the differing chemical and mineralogical composition of the dusts under investigation. Huang *et al.*[22] have studied the RH-dependence of SO_2 uptake on Asian Mineral Dust (AMD), ATD and Tengger Desert Dust (TDD); they observe a decrease in SO_2 uptake with increasing RH on AMD, but the opposite on ATD and TDD. Moreover, the data presented by Huang *et al.* show that on each type of dust investigated, a change in the behavior of SO_2 uptake occurs around 30% RH, in agreement with our observations for the v-dust samples. Consistently, the formation of a water monolayer is observed at 28 ± 2% RH on the 40–80 μm fraction of ATD.[60] Li *et al.*[61] investigated the uptake of SO_2 by $CaCO_3$ in the presence of O_3, and did not observe a dependence of the initial SO_2 uptake coefficient on RH. However, they report an increase of $\gamma_{SS,BET}$ from 2×10^{-9} at 5% RH to 2×10^{-8} at 60% RH, although the variation in SO_2 uptake between these RH values is not reported. The latter value of 2×10^{-8} at 60% RH is consistent with our value of roughly 4.5×10^{-8} between 50% and 72% RH.

4. Concluding remarks

We investigated the heterogeneous interaction of SO_2 with four Icelandic v-dust samples under atmospherically relevant conditions, with and without UV light. The uptake of SO_2 on the v-dusts is time-dependent both in the dark and under UV irradiation. In particular, a substantial quantity of SO_2 is taken up initially in a transient process, with N_S values measured in the dark on the order of 10^{13} molecules cm^{-2} using the S_{BET} surface. After several hours of exposure to SO_2, the v-dust surface saturates/deactivates, probably due to the formation of low volatility surface products such as SO_3^{2-} and SO_4^{2-}. Following SO_2 uptake in the dark, UV irradiation of the v-dust surfaces promotes an additional consumption of SO_2, with N_S values measured under UV light on the order of 10^{14} molecules cm^{-2} using S_{BET}. The photo-enhanced removal of SO_2, characterized by $N_{S,light}/N_{S,dark}$, is correlated with the surface Ti/Si composition, the UV irradiance intensity and RH. Based on our experimental observations, a general equation is proposed to extrapolate the amplification of SO_2 removal by a photo-induced heterogeneous process as a function of the atmospheric parameters studied. The proposed parametrization concerns the results of the current study, and requires validation with more experiments and samples before general application. We attribute the photo-enhanced heterogeneous uptake of SO_2 to the formation of active surface species on Ti-containing surface sites and/or to photochemical reactions of intermediate surface groups. Both processes promote the uptake and transformation of SO_2 into final surface products such as SO_4^{2-} and HSO_4^- species. However, the clarification of the reaction mechanism requires more studies, preferably through real-time monitoring of surface species both in the dark and under UV light.

This work has implications for atmospheric models aiming to simulate the removal of SO_2 by resuspended volcanic material, and to elucidate the importance of heterogeneous processes both under nighttime and daytime tropospheric conditions. Based on our results, we anticipate that the impact of SO_2 heterogeneous chemistry is more important on irradiated volcanic particles. Indeed, under tropospheric conditions, the photo-enhanced removal of SO_2 evidenced in the present study is up to seven times higher than under dark conditions. Climate or chemical transport models should therefore include diurnal profiles of SO_2 uptake by volcanic particles to improve representation of the sulfur budget, and of its evolution in the atmosphere following an eruption. However, to the best of our knowledge there are no modeling studies incorporating the heterogeneous removal of SO_2 on solid particles of volcanic origin in the troposphere.

In a recent study, Zhu *et al.*[62] performed aerosol-climate model simulations to estimate the impact of the heterogeneous removal of SO_2 on volcanic ash particles in the stratosphere. Specifically, they compared the results of model simulations which included the uptake of SO_2 on ash with satellite and aircraft observations following the 2014 Kelud eruption. The best match of the model results to the observational data was achieved using γ and N_S values (3×10^{-3} and 3×10^{16} molecules cm^{-2}, respectively), normalized to geometric surface area of the ash particles, of the same order of magnitude as those measured in laboratory experiments in the absence of UV light and at room temperature. However, note that SO_2 uptake normalized to geometric surface area represents an upper limit and may exceed by more than one order of magnitude the SO_2 uptake normalized to the true surface area calculated from S_{BET}.[20] The resulting model simulations of Zhu *et al.*[62] reveal for the first time that heterogeneous reaction of SO_2 with volcanic ash could remove up to 43% more sulfur from the stratosphere within two months of the eruption. However, it should be mentioned that these authors did not include any daytime photo-induced loss of SO_2 on volcanic ash, a process that could be important under stratospheric conditions where short wavelength radiation is present (UV-A and UV-B), as highlighted by the present study. The absence of these photo-processes in their model might contribute to the relatively high γ and N_S values needed by Zhu *et al.*[62] to match simulations with observations.

Building on recent advances in laboratory and model studies, there is still much to learn regarding controls on SO_2 uptake by volcanic ash/dust, the underlying reaction mechanisms, and the potential atmospheric and climate impacts. Laboratory temperature-dependent studies are necessary to provide uptake coefficient and surface coverage values under relevant tropospheric/stratospheric conditions. The inclusion of diurnal heterogeneous removal of SO_2 in both tropospheric and stratospheric model simulations is also recommended to better capture the photo-induced variation in heterogeneous SO_2 loss, evidenced and characterized in this work.

Funding sources

This work was achieved in the frame of Labex CaPPA, funded by ANR through the PIA under contract ANR-11-LABX-0005-01, and CPER CLIMIBIO project, both funded by the Hauts-de-France Regional Council and the European Regional Development Fund (ERDF).

Author contributions

The manuscript was written through contributions of all authors. All authors have given approval to the final version of the manuscript.

Conflicts of interest

There are no conflicts to declare.

Acknowledgements

The authors acknowledge Mr V. Gaudion and Dr M. Zeineddine (CERI EE, IMT Nord Europe) for their assistance in the lab. Mr E. Tison (CERI EE, IMT Nord Europe) is gratefully acknowledged for providing the SO_2 analyzer, and Dr Pavla Dagsson-Waldhauserova (University of Iceland) for providing the volcanic dust samples. We thank P. Eloy for performing the XPS analysis. JL acknowledges invaluable discussions with Dr D. Marchione (Università degli Studi di Perugia, Italy) and Dr A. Rosu-Finsen (University College London, UK). This work was achieved in the frame of Labex CaPPA, funded by ANR through the PIA under contract ANR-11-LABX-0005-01, and CPER CLIMIBIO project, both funded by the Hauts-de-France Regional Council and the European Regional Development Fund (ERDF). JL acknowledges support from the Labex CaPPA, CPER CLIMIBIO, the Hauts-de-France Regional Council, and IMT Nord Europe (project IRAPAQ) for post-doctoral fellowships. EM acknowledges the Leverhulme Trust and Isaac Newton Trust for an Early Career Fellowship.

References

1 A. J. Durant, C. Bonadonna and C. J. Horwell, Atmospheric and Environmental Impacts of Volcanic Particulates, *Elements*, 2010, **6**, 235–240.
2 M. O. Andreae, in *World Survey of Climatology*, ed. A. Henderson-Sellers, Elsevier, 1995, vol. 16, pp. 347–398.
3 T. Thordarson and Á. Höskuldsson, Postglacial volcanism in Iceland, *Jokull*, 2008, **58**, 197–228.
4 A. Stohl, A. J. Prata, S. Eckhardt, L. Clarisse, A. Durant, S. Henne, N. I. Kristiansen, A. Minikin, U. Schumann, P. Seibert, K. Stebel, H. E. Thomas, T. Thorsteinsson, K. Tørseth and B. Weinzierl, Determination of time- and height-resolved volcanic ash emissions and their use for quantitative ash dispersion modeling: the 2010 Eyjafjallajökull eruption, *Atmos. Chem. Phys.*, 2011, **11**, 4333–4351.
5 O. Arnalds, P. Dagsson-Waldhauserova and H. Olafsson, The Icelandic volcanic aeolian environment: Processes and impacts — A review, *Aeolian Res.*, 2016, **20**, 176–195.
6 F. Beckett, A. Kylling, G. Sigurðardóttir, S. von Löwis and C. Witham, Quantifying the mass loading of particles in an ash cloud remobilized from tephra deposits on Iceland, *Atmos. Chem. Phys.*, 2017, **17**, 4401–4418.
7 D. Đorđević, I. Tošić, S. Sakan, S. Petrović, J. Đuričić-Milanković, D. C. Finger and P. Dagsson-Waldhauserová, Can Volcanic Dust Suspended From Surface Soil and Deserts of Iceland Be Transferred to Central Balkan Similarly to African Dust (Sahara)?, *Front. Earth Sci.*, 2019, **7**, 142.
8 A. Yoshida, N. Moteki, S. Ohata, T. Mori, R. Tada, P. Dagsson-Waldhauserová and Y. Kondo, Detection of light-absorbing iron oxide particles using a modified single-particle soot photometer, *Aerosol Sci. Technol.*, 2016, **50**, 1–4.

9 E. J. Highwood and D. S. Stevenson, Atmospheric impact of the 1783–1784 Laki Eruption: Part II Climatic effect of sulphate aerosol, *Atmos. Chem. Phys.*, 2003, **3**, 1177–1189.
10 D. S. Stevenson, C. E. Johnson, E. J. Highwood, V. Gauci, W. J. Collins and R. G. Derwent, Atmospheric impact of the 1783–1784 Laki eruption: Part I Chemistry modelling, *Atmos. Chem. Phys.*, 2003, **3**, 487–507.
11 J.-P. Vernier, T. D. Fairlie, T. Deshler, M. Natarajan, T. Knepp, K. Foster, F. G. Wienhold, K. M. Bedka, L. Thomason and C. Trepte, In situ and space-based observations of the Kelud volcanic plume: The persistence of ash in the lower stratosphere, *J. Geophys. Res.: Atmos.*, 2016, **121**, 11104–111118.
12 A. Vogel, S. Diplas, A. J. Durant, A. S. Azar, M. F. Sunding, W. I. Rose, A. Sytchkova, C. Bonadonna, K. Krüger and A. Stohl, Reference data set of volcanic ash physicochemical and optical properties, *J. Geophys. Res.: Atmos.*, 2017, **122**, 9485–9514.
13 C. Oppenheimer, P. Francis, M. Burton, A. J. H. Maciejewski and L. Boardman, Remote measurement of volcanic gases by Fourier transform infrared spectroscopy, *Appl. Phys. B*, 1998, **67**, 505–515.
14 D. E. Hunton, A. A. Viggiano, T. M. Miller, J. O. Ballenthin, J. M. Reeves, J. C. Wilson, S.-H. Lee, B. E. Anderson, W. H. Brune, H. Harder, J. B. Simpas and N. Oskarsson, In-situ aircraft observations of the 2000 Mt. Hekla volcanic cloud: Composition and chemical evolution in the Arctic lower stratosphere, *J. Volcanol. Geotherm. Res.*, 2005, **145**, 23–34.
15 K. P. Heue, C. A. M. Brenninkmeijer, A. K. Baker, A. Rauthe-Schöch, D. Walter, T. Wagner, C. Hörmann, H. Sihler, B. Dix, U. Frieß, U. Platt, B. G. Martinsson, P. F. J. van Velthoven, A. Zahn and R. Ebinghaus, SO_2 and BrO observation in the plume of the Eyjafjallajökull volcano 2010: CARIBIC and GOME-2 retrievals, *Atmos. Chem. Phys.*, 2011, **11**, 2973–2989.
16 M. Höpfner, C. D. Boone, B. Funke, N. Glatthor, U. Grabowski, A. Günther, S. Kellmann, M. Kiefer, A. Linden, S. Lossow, H. C. Pumphrey, W. G. Read, A. Roiger, G. Stiller, H. Schlager, T. von Clarmann and K. Wissmüller, Sulfur dioxide (SO_2) from MIPAS in the upper troposphere and lower stratosphere 2002–2012, *Atmos. Chem. Phys.*, 2015, **15**, 7017–7037.
17 H. K. Carlsen, U. Valdimarsdóttir, H. Briem, F. Dominici, R. G. Finnbjornsdottir, T. Jóhannsson, T. Aspelund, T. Gislason and T. Gudnason, Severe volcanic SO(2) exposure and respiratory morbidity in the Icelandic population - a register study, *Environ. Health: Global Access Sci. Source*, 2021, **20**, 23.
18 H. K. Carlsen, E. Ilyinskaya, P. J. Baxter, A. Schmidt, T. Thorsteinsson, M. A. Pfeffer, S. Barsotti, F. Dominici, R. G. Finnbjornsdottir, T. Jóhannsson, T. Aspelund, T. Gislason, U. Valdimarsdóttir, H. Briem and T. Gudnason, Increased respiratory morbidity associated with exposure to a mature volcanic plume from a large Icelandic fissure eruption, *Nat. Commun.*, 2021, **12**, 2161.
19 J. Penner, Three ways through the soot, sulfates and dust, *Nature*, 2019, **570**, 158–159.
20 J. N. Crowley, M. Ammann, R. A. Cox, R. G. Hynes, M. E. Jenkin, A. Mellouki, M. J. Rossi, J. Troe and T. J. Wallington, Evaluated kinetic and photochemical data for atmospheric chemistry: Volume V – heterogeneous reactions on solid substrates, *Atmos. Chem. Phys.*, 2010, **10**, 9059–9223.
21 L. Zhou, W. Wang, Y. Gai and M. Ge, Knudsen cell and smog chamber study of the heterogeneous uptake of sulfur dioxide on Chinese mineral dust, *J. Environ. Sci.*, 2014, **26**, 2423–2433.
22 L. Huang, Y. Zhao, H. Li and Z. Chen, Kinetics of Heterogeneous Reaction of Sulfur Dioxide on Authentic Mineral Dust: Effects of Relative Humidity and Hydrogen Peroxide, *Environ. Sci. Technol.*, 2015, **49**, 10797–10805.
23 E. C. Maters, P. Delmelle, M. J. Rossi and P. M. Ayris, Reactive Uptake of Sulfur Dioxide and Ozone on Volcanic Glass and Ash at Ambient Temperature, *J. Geophys. Res.: Atmos.*, 2017, **122**, 10077–10088.
24 D. Urupina, J. Lasne, M. N. Romanias, V. Thiery, P. Dagsson-Waldhauserova and F. Thevenet, Uptake and surface chemistry of SO2 on natural volcanic dusts, *Atmos. Environ.*, 2019, **217**, 116942.
25 D. Urupina, M. N. Romanias and F. Thevenet, How Relevant Is It to Use Mineral Proxies to Mimic the Atmospheric Reactivity of Natural Dust Samples? A Reactivity Study Using SO2 as Probe Molecule, *Minerals*, 2021, **11**, 282.
26 M. N. Romanias, Y. Ren, B. Grosselin, V. Daële, A. Mellouki, P. Dagsson-Waldhauserova and F. Thevenet, Reactive uptake of NO_2 on volcanic particles: A possible source of HONO in the atmosphere, *J. Environ. Sci.*, 2020, **95**, 155–164.
27 M. J. Genet, C. C. Dupont-Gillain and P. G. Rouxhet, XPS analysis of biosystems and biomaterials, *J. Environ. Sci.*, 2008, 177–309.
28 J. Lasne, M. N. Romanias and F. Thevenet, Ozone Uptake by Clay Dusts under Environmental Conditions, *ACS Earth Space Chem.*, 2018, **2**, 904–914.
29 J. C. Barnard, E. G. Chapman, J. D. Fast, J. R. Schmelzer, J. R. Slusser and R. E. Shetter, An evaluation of the FAST-J photolysis algorithm for predicting nitrogen dioxide photolysis rates under clear and cloudy sky conditions, *Atmos. Environ.*, 2004, **38**, 3393–3403.
30 B. Bohn, F. Rohrer, T. Brauers and A. Wahner, Actinometric measurements of NO_2 photolysis frequencies in the atmosphere simulation chamber SAPHIR, *Atmos. Chem. Phys.*, 2005, **5**, 493–503.
31 C. Topaloglou, S. Kazadzis, A. F. Bais, M. Blumthaler, B. Schallhart and D. Balis, NO_2 and HCHO photolysis frequencies from irradiance measurements in Thessaloniki, Greece, *Atmos. Chem. Phys.*, 2005, **5**, 1645–1653.
32 T. Huthwelker, M. Ammann and T. Peter, The Uptake of Acidic Gases on Ice, *Chem. Rev.*, 2006, **106**, 1375–1444.
33 M. T. C. Martins-Costa, J. M. Anglada, J. S. Francisco and M. F. Ruiz-López, Photochemistry of SO2 at the Air–Water Interface: A Source of OH and HOSO Radicals, *J. Am. Chem. Soc.*, 2018, **140**, 12341–12344.

34 M. N. Romanias, A. El Zein and Y. Bedjanian, Heterogeneous Interaction of H_2O_2 with TiO_2 Surface Under Dark and UV Light Irradiation Conditions, *J. Phys. Chem. A*, 2012, **116**, 8191–8200.

35 M. N. Romanias, Y. Bedjanian, A. M. Zaras, A. Andrade-Eiroa, R. Shahla, P. Dagaut and A. Philippidis, Mineral Oxides Change the Atmospheric Reactivity of Soot: NO_2 Uptake Under Dark and UV Irradiation Conditions, *J. Phys. Chem. A*, 2013, **117**, 12897–12911.

36 M. J. Tang, R. A. Cox and M. Kalberer, Compilation and evaluation of gas phase diffusion coefficients of reactive trace gases in the atmosphere: volume 1. Inorganic compounds, *Atmos. Chem. Phys.*, 2014, **14**, 9233–9247.

37 S. Brunauer, P. H. Emmett and E. Teller, Adsorption of Gases in Multimolecular Layers, *J. Am. Chem. Soc.*, 1938, **60**, 309–319.

38 J. M. Herrmann, Heterogeneous photocatalysis: state of the art and present applications, *Top. Catal.*, 2005, **34**, 49–65.

39 H. Chen, C. E. Nanayakkara and V. H. Grassian, Titanium Dioxide Photocatalysis in Atmospheric Chemistry, *Chem. Rev.*, 2012, **112**, 5919–5948.

40 C. George, M. Ammann, B. D'Anna, D. J. Donaldson and S. A. Nizkorodov, Heterogeneous Photochemistry in the Atmosphere, *Chem. Rev.*, 2015, **115**, 4218–4258.

41 C. Anastasio, M. Hoffmann, P. Klán and J. Sodeau, in *The Science of Solar System Ices*, ed. M. S. Gudipati and J. Castillo-Rogez, Springer, New York, NY, 2013, pp. 583–644, DOI: DOI: 10.1007/978-1-4614-3076-6_18.

42 L. Dogliotti and E. Hayon, Flash photolysis study of sulfite, thiocyanate, and thiosulfate ions in solution, *J. Phys. Chem.*, 1968, **72**, 1800–1807.

43 P. Neta and R. E. Huie, Free-Radical Chemistry of Sulfite, *Environ. Health Perspect.*, 1985, **64**, 209–217.

44 J. Schneider, M. Matsuoka, M. Takeuchi, J. Zhang, Y. Horiuchi, M. Anpo and D. W. Bahnemann, Understanding TiO2 Photocatalysis: Mechanisms and Materials, *Chem. Rev.*, 2014, **114**, 9919–9986.

45 A. E. Zein, M. N. Romanias and Y. Bedjanian, Heterogeneous Interaction of H_2O_2 with Arizona Test Dust, *J. Phys. Chem. A*, 2014, **118**, 441–448.

46 M. N. Romanias, A. El Zein and Y. Bedjanian, Reactive uptake of HONO on aluminium oxide surface, *J. Photochem. Photobiol., A*, 2012, **250**, 50–57.

47 M. N. Zeineddine, M. N. Romanias, V. Gaudion, V. Riffault and F. Thevenet, Heterogeneous Interaction of Isoprene with Natural Gobi Dust, *ACS Earth Space Chem.*, 2017, **1**, 236–243.

48 M. N. Zeineddine, M. N. Romanias, V. Riffault and F. Thévenet, Heterogeneous Interaction of Various Natural Dust Samples with Isopropyl Alcohol as a Probe VOC, *J. Phys. Chem. A*, 2018, **122**, 4911–4919.

49 J. Shang, J. Li and T. Zhu, Heterogeneous reaction of SO_2 on TiO_2 particles, *Sci. China: Chem.*, 2010, **53**, 2637–2643.

50 M. Tang, X. Huang, K. Lu, M. Ge, Y. Li, P. Cheng, T. Zhu, A. Ding, Y. Zhang, S. Gligorovski, W. Song, X. Ding, X. Bi and X. Wang, Heterogeneous reactions of mineral dust aerosol: implications for tropospheric oxidation capacity, *Atmos. Chem. Phys.*, 2017, **17**, 11727–11777.

51 M. N. Romanias, M. N. Zeineddine, V. Riffault and F. Thevenet, Isoprene Heterogeneous Uptake and Reactivity on TiO2: A Kinetic and Product Study, *Int. J. Chem. Kinet.*, 2017, **49**, 773–788.

52 N. Joshi, M. N. Romanias, V. Riffault and F. Thevenet, Investigating water adsorption onto natural mineral dust particles: Linking DRIFTS experiments and BET theory, *Aeolian Res.*, 2017, **27**, 35–45.

53 M. Tang, D. J. Cziczo and V. H. Grassian, Interactions of Water with Mineral Dust Aerosol: Water Adsorption, Hygroscopicity, Cloud Condensation, and Ice Nucleation, *Chem. Rev.*, 2016, **116**, 4205–4259.

54 J. Park, M. Jang and Z. Yu, Heterogeneous Photo-oxidation of SO2 in the Presence of Two Different Mineral Dust Particles: Gobi and Arizona Dust, *Environ. Sci. Technol.*, 2017, **51**, 9605–9613.

55 Y. Dupart, S. M. King, B. Nekat, A. Nowak, A. Wiedensohler, H. Herrmann, G. David, B. Thomas, A. Miffre, P. Rairoux, B. D'Anna and C. George, Mineral dust photochemistry induces nucleation events in the presence of SO_2, *Proc. Natl. Acad. Sci.*, 2012, 12297, DOI: 10.1073/pnas.1212297109%J.

56 J. W. Adams, D. Rodriguez and R. A. Cox, The uptake of SO_2 on Saharan dust: a flow tube study, *Atmos. Chem. Phys.*, 2005, **5**, 2679–2689.

57 J. Y. Park and M. Jang, Heterogeneous photooxidation of sulfur dioxide in the presence of airborne mineral dust particles, *RSC Adv.*, 2016, **6**, 58617–58627.

58 Z. Yu, M. Jang and J. Park, Modeling atmospheric mineral aerosol chemistry to predict heterogeneous photooxidation of SO2, *Atmos. Chem. Phys.*, 2017, **17**, 10001–10017.

59 Y. Dupart, *Impact de la chimie des poussières minérales sur la photochimie atmosphérique*, PhD thesis, Université de Lyon 1, p. 2012.

60 S. Ibrahim, M. N. Romanias, L. Y. Alleman, M. N. Zeineddine, G. K. Angeli, P. N. Trikalitis and F. Thevenet, Water Interaction with Mineral Dust Aerosol: Particle Size and Hygroscopic Properties of Dust, *ACS Earth Space Chem.*, 2018, **2**, 376–386.

61 L. Li, Z. M. Chen, Y. H. Zhang, T. Zhu, J. L. Li and J. Ding, Kinetics and mechanism of heterogeneous oxidation of sulfur dioxide by ozone on surface of calcium carbonate, *Atmos. Chem. Phys.*, 2006, **6**, 2453–2464.

62 Y. Zhu, O. B. Toon, E. J. Jensen, C. G. Bardeen, M. J. Mills, M. A. Tolbert, P. Yu and S. Woods, Persisting volcanic ash particles impact stratospheric SO_2 lifetime and aerosol optical properties, *Nat. Commun.*, 2020, **11**, 4526.